

BRAF^{V600E}-induced KRT19 expression in thyroid cancer promotes lymph node metastasis via EMT

XUHONG WANG¹, XIAOQIN XU², CHEN PENG¹, YANCHAO QIN¹,
TAIHU GAO¹, JIEXIAN JING² and HONGCAI ZHAO¹

Departments of ¹Head and Neck Surgery, and ²Etiology, Shanxi Cancer Hospital, Taiyuan, Shanxi 030013, P.R. China

Received July 17, 2018; Accepted April 15, 2019

DOI: 10.3892/ol.2019.10360

Abstract. Keratin 19 (KRT19) is a type I cytokeratin that serves an important role in multiple types of cancer; however, little is known regarding its role in thyroid cancer. Therefore, the aim of the current study was to investigate the role of KRT19 in thyroid cancer. Using The Cancer Genome Atlas database, the expression and clinical significance of KRT19 in thyroid cancer tissues were investigated. The effect of KRT19 in thyroid cancer cell lines was also investigated *in vitro*. The results demonstrated that KRT19 expression was higher in thyroid cancer when compared with normal thyroid tissues, and was associated with lymph node metastasis, tumor stage and tumor-node-metastasis stage. Knockdown of KRT19 inhibited the proliferation and migration of thyroid cancer cell lines. In addition, increased KRT19 expression was observed only in tumors harboring the B-Raf Proto-Oncogene, Serine/Threonine Kinase (BRAF)^{V600E} mutation, and BRAF^{V600E} overexpression induced KRT19 expression. Furthermore, KRT19 exerted its phenotype via promoting epithelial-mesenchymal transition (EMT). In conclusion, the results of the current study suggest that BRAF^{V600E}-induced KRT19 expression may promote thyroid cancer metastasis via EMT.

Introduction

Thyroid cancer is the most commonly diagnosed type of head and neck cancer (1). Differentiated thyroid cancer is the most common type of thyroid cancer, which accounts for >95% of all cases (2). Due to increased use of diagnostic imaging and surveillance techniques over the last 30 years, with the exception of Africa, the incidence rates of thyroid cancer have continued to increase worldwide, and it accounted for

3.4% of all cancers in the USA in 2017 (3,4). The B-Raf Proto-Oncogene, Serine/Threonine Kinase (BRAF)^{V600E} mutation is one of the most common mutations observed in thyroid cancer.

Keratins are the intermediate filament (IF)-forming proteins in epithelial cells and have been long and extensively used as immunohistochemical markers for the pathological diagnosis of tumors (5). The keratin 19 (KRT19) gene, located at chromosome17q21.2, encodes for the cytokeratin (CK)19 protein, CK-19, which is an acidic protein type I CK (6). KRT19 has been studied as a prognostic marker and has been found to exert specific biological roles in numerous types of cancer, including hepatocellular carcinoma, pancreatic neuroendocrine tumors and potentially HER2-positive breast cancer (7-10). However, its role in thyroid cancer is currently unclear, therefore, the aim of the present study was to examine the role of KRT19 in thyroid cancer cell lines, and further explore the potential mechanism of KRT19 overexpression. KRT19 expression was observed to be higher in thyroid cancer samples when compared with normal thyroid tissue samples and therefore, may function as a potential oncogene that promotes thyroid cancer cell proliferation and migration *in vitro*. In addition, the present study, to the best of our knowledge, reported for the first time that the BRAF^{V600E} mutation may contribute to the oncogenic function of KRT19. This suggests that KRT19 and BRAF^{V600E} may serve a role in epithelial-mesenchymal transition (EMT).

Materials and methods

Data sources. The Cancer Genome Atlas (TCGA), Level 3 thyroid cancer data were first downloaded from UCSC Xena (<https://xenabrowser.net/datapages/>). The TCGA Thyroid Cancer (TCGA_THCA) dataset (ID, TCGA.THCA.sampleMap/HiSeqV2; version 20171013) contained the following information on 572 patients with thyroid cancer: Tumor-Node-Metastasis (TNM) stage (11), age, grading, pathology type (follicular subtype, classical subtype and tall cell subtype) and other clinical parameters. The TCGA_THCA dataset was produced using Illumina HiSeq (Illumina, Inc.), consisted of 59 normal thyroid tissues and 505 cancer tissues, and was analyzed using the unit log₂(count+1), and 'count' was considered as the second-generation sequencing RSEM normalized count (12). For mutation analysis, the

Correspondence to: Dr Hongcai Zhao, Department of Head and Neck Surgery, Shanxi Cancer Hospital, 3 Zhigongxinjie Street, Taiyuan, Shanxi 030013, P.R. China
E-mail: zhao-hongcai@outlook.com

Key words: thyroid cancer, B-Raf Proto-Oncogene, Serine/Threonine Kinase^{V600E}, keratin 19, epithelial-mesenchymal-transition, metastasis

TCGA thyroid carcinoma somatic mutation (broad automated) (ID, TCGA.THCA.sampleMap/mutation_broad; version 20170908,) dataset, consisting of 504 samples, was used. Analysis of gene set enrichment was performed according to the Gene Set Enrichment Analysis (GSEA) instructions (13,14). Gene expression analysis results from 10 samples exhibiting the highest levels of KRT19 expression, together with the 10 samples with the lowest levels of KRT19 expression were submitted to GSEA for analysis.

Cell lines, culture conditions, small interfering (si)RNA, plasmids and transfection. The thyroid cancer cell line, 8505C was obtained from Sigma-Aldrich (Merck KGaA; cat. no. 94090184), the cancer cell line, BHT101, was obtained from the Leibniz Institute DSMZ-German Collection of Microorganisms and Cell Cultures (cat. no. ACC 279), Phoenix cells were obtained from the American Type Culture Collection (ATCC; cat. no. CRL-3213). 8505C and BHT101 cells were cultured in Eagle's minimum essential medium (ATCC; cat. no. 30-2003) and Phoenix cells in Dulbecco's modified Eagle's medium (Thermo Fisher Scientific, Inc.; cat. no. 12491-015) supplemented with 10% fetal bovine serum (FBS; cat. no. 10500064; Gibco; Thermo Fisher Scientific, Inc.) and penicillin/streptomycin and cultured in a humidified incubator at 37°C and 5% CO₂.

Transfection was performed according to the manufacturer's siRNA sequence transfection protocol for Lipofectamine RNAiMAX (30 pmol siRNA per every 6 well plate well; cat. no. 13778075; Thermo Fisher Scientific, Inc.) and the plasmid Lipofectamine 2000 (2 µg plasmid DNA per every 6 well plate well; cat. no. 11668027; Thermo Fisher Scientific, Inc.) protocol. The wild type (WT) BRAF^{WT} (pcDNA3.1, cat. no. 40775; Addgene, Inc.) with its empty vector were transfected to the cells followed by Lipofectamine 2000 instruction and mutant BRAF^{V600E} (pBabe, cat. no. 15269; Addgene, Inc.) with its empty vector were transfected into retrovirus packaging phoenix cells (with an VSV.G envelope plasmid; cat. no. 14888; Addgene, Inc.), after 48 h culturing the virus supernatant was harvested and filtered. The retrovirus was subsequently introduced into the phoenix cells by spin infection at 1,200 x g for 90 min at 32°C. A non-targeting RNA interference sequence (10 µM; Ambion; Thermo Fisher Scientific, Inc.) was used as a negative control (5'-CCT AAGGTTAAGTCGCCCTCGCTC-3') for KRT19 siRNA experiments (targeting sequence, 5'-AACCATGAGGAG GAAATCA-3') (15). Transfection efficiency was evaluated by reverse transcription-quantitative PCR (RT-qPCR) and western blot analyses 48 h after transfection.

RNA preparation and RT-qPCR. Total RNA was extracted from cultured 8505C and BHT101 cells using TRIzol reagent (Invitrogen; Thermo Fisher Scientific, Inc.). For reverse transcription, 1,000 ng total RNA was reverse transcribed to produce a final volume of 20 µl cDNA using a Reverse Transcription kit (cat. no. RR036A; Takara Biotechnology, Co., Ltd.), according to the manufacturer's protocols. RT-qPCR analyses were performed using SYBR Select Master Mix (cat. no. 4472908; Applied Biosystems; Thermo Fisher Scientific, Inc.), according to the manufacturer's protocols. The RT-qPCR primers for KRT19 were

as follows: Forward, 5'-AACGGCGAGCTAGAGGTGA-3', and reverse, 5'-GGATGGTTCGTGTAGTAGTGGC-3', the primers for BRAF^{WT}/BRAF^{V600E} were forward, 5'-AATACA CCAGCAAGCTAGATGC-3', and reverse, 5'-AATCAGTTC CGTTCGCCAGAG-3'. β-actin was used as the reference gene with the following primer sequences: Forward, 5'-CAT GTACGTTGCTATCCAGGC-3' and reverse, 5'-CTCCTT AATGTCACGCACGAT-3'. RT-qPCR data was collected using the QuantStudio™ 6 Flex Real-Time PCR System (Applied Biosystems; Thermo Fisher Scientific, Inc.) and RT-qPCR thermocycling conditions consisted of an initial denaturation step at 95°C for 10 min, followed by 40 cycles of 92°C for 15 sec and 60°C for 1 min. Each sample was run in triplicate and the relative expression of the target gene was calculated and normalized relative to β-actin using the 2^{-ΔΔC_q} method (16) in Excel 16.18 software (Microsoft Corporation).

Protein preparation and western blot analysis. Whole cells were lysed on ice with RIPA buffer (cat. no. P0013; Beyotime Institute of Biotechnology), and a bicinchoninic acid assay kit was used to quantify the protein concentration. Equal quantities (15 µg) of protein were loaded onto 12% SDS PAGE gels. Following separation, protein samples were transferred to nitrocellulose membranes. The membranes were blocked in 2% bovine serum albumin (cat. no. A4737; Sigma-Aldrich; Merck KGaA) in Tris-buffered saline and Tween 20 (TBST) for 1 h at room temperature and incubated with antibodies at 4°C overnight. The membranes were then washed in TBST and incubated with HRP-coupled secondary antibodies for 2 h at room temperature. After that membranes were treated with enhanced chemiluminescence western blotting substrate (Pierce; cat. no., 32106) at room temperature for 1 min, X-ray films (CL-XPosure™ Film; cat. no. 34090, Thermo Fisher Scientific, Inc.) were used for detecting the blots. All experiments were repeated in triplicate and the antibodies are presented in Table I.

Cell proliferation and migration assays. The Cell Counting Kit-8 (CCK8; cat. no. CK04; Dojindo Molecular Technologies, Inc.) was used to determine the cell proliferation rate. Cells were seeded in 96-well plates at a density of 2,000 cells/well (100 µl total volume), and the absorbance was measured at a wavelength of 450 nm using an ELx800 Universal Microplate Reader (Norgen Biotek Corp.), according to the manufacturer's protocols. Each experiment was repeated in quadruplicate at 0, 24, 48, 72 and 96 h.

For migration assays, transfected cells (40,000 cells/well; 100 µl total volume) were seeded in the upper chamber of Transwell assay inserts (8-mm pores; EMD Millipore) containing 200 µl serum-free media. The lower chambers were filled with media containing 10% FBS. Following incubation for 24 h, cells on the filter surface were fixed with 90% methanol (-20°C) for 10 min and then stained with crystal violet for 10 min at room temperature. Images were captured using a light inverted microscope (magnification, x40; Axio Observer; Carl Zeiss AG) and cell migration was assessed by counting the number of stained cells in five random fields of view/filter for each group. Experiments were repeated in triplicate.

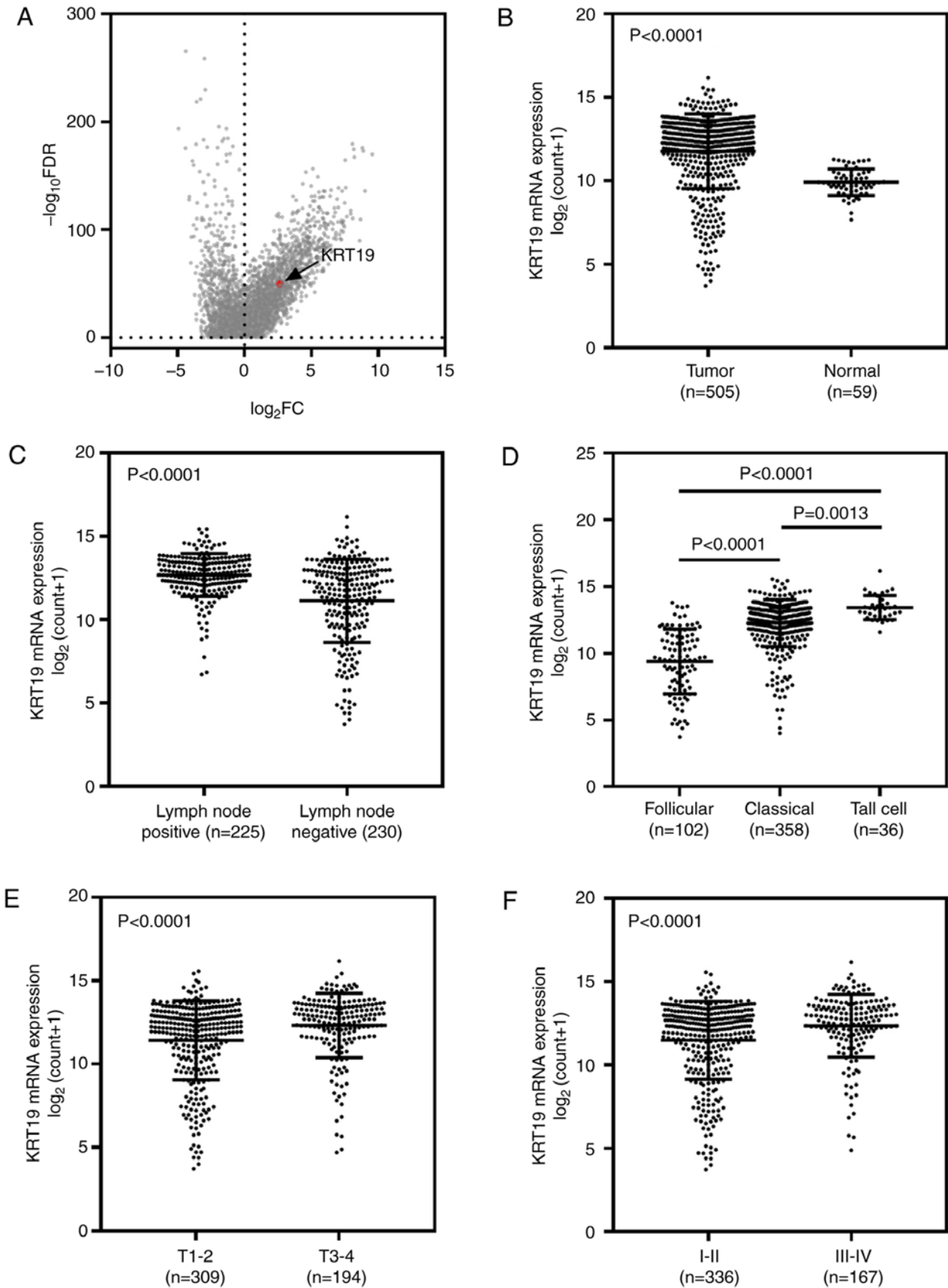


Figure 1. The TCGA_THCA dataset was used for clinical analyses. (A) A volcano plot showing the expression of 20,530 genes from the THCA dataset grouped by tumor vs. normal. KRT19 is at an upregulated position. (B) Increased KRT19 expression is observed in THCA when compared with normal tissues. (C) KRT19 expression is associated with lymph node metastasis. The lymph node positive group exhibited higher KRT19 expression levels. (D) The expression of KRT19 in different histological subtypes; the follicular subtype exhibited the lowest KRT19 expression levels, while the tall cell subtype exhibited the highest expression levels. (E) Increased primary tumor size was associated with higher KRT19 expression. (F) KRT19 expression was associated with TNM stage, more advanced TNM stage and high KRT19 expression. TCGA, The Cancer Genome Atlas Network; THCA, thyroid cancer; KRT19, keratin 19; TNM, tumor-node-metastasis; FDR, false discovery rate; FC, fold change (tumor vs. normal).

Table I. Antibody list.

Antibody target	Supplier and catalogue number	Host	Dilution
KRT19	Abcam; cat. no., ab15463	Rabbit	1:200
β -actin	Cell Signaling Technology, Inc.; cat. no., 8H10D10	Mouse	1:500
BRAF ^{V600E}	Sigma-Aldrich; Merck KGaA; cat. no., SAB5600047	Rabbit	1:300
E-cadherin	Cell Signaling Technology, Inc.; cat. no., 24E10	Rabbit	1:500
N-cadherin	Cell Signaling Technology, Inc.; cat. no., D4R1H	Rabbit	1:500
HRP-coupled Anti-rabbit IgG	Cell Signaling Technology, Inc.; cat. no., 14708		1:1,000
HRP-coupled Anti-mouse IgG	Cell Signaling Technology, Inc.; cat. no., 14709		1:1,000

KRT19, keratin-19; BRAF, B-Raf proto-oncogene, serine/threonine kinase.

Table II. Clinical analysis in TCGA_THCA.

Characteristics	Number of patients	Percentage (%)	P-value
Age (years)			0.010
<60	385	76.2	
\geq 60	120	23.8	
Sex			0.871
Male	136	26.9	
Female	369	73.1	
Primary tumor			<0.001
T1-2	310	61.4	
T3-4	195	38.6	
Lymph node metastasis			<0.001
Positive	225	49.5	
Negative	230	50.5	
TNM stage			<0.001
I-II	336	66.8	
III-IV	167	33.2	
Metastasis			0.780
Positive	282	96.9	
Negative	9	3.1	

TNM, tumor-node-metastasis; THCA, thyroid cancer; TCGA, The Cancer Genome Atlas Network.

Flow cytometry analysis. Apoptosis was analyzed by flow cytometry using an Annexin V-fluorescein isothiocyanate (FITC) Apoptosis Detection kit (BD Biosciences) with propidium iodide (PI), according to the manufacturer's instructions. Briefly, cells were first washed and resuspended at a concentration of 1×10^6 cells/ml. The cells were then incubated with Annexin V-FITC (1:20 dilution) at room temperature in the dark for 20 min and after that, PI (1:20 dilution) was added. The samples were immediately analyzed using a FACScan flow cytometer (BD Biosciences). FlowJo software (version 10; FlowJo LLC) was used for data analysis. Each assay was performed in triplicate.

Statistical analysis. SPSS Statistics 20.0 software (IBM Corp.) and GraphPad Prism 7.04 (GraphPad Software, Inc.)

software were used for statistical analyses and the production of graphs. Data are presented as the mean \pm standard deviation, and were analyzed using a Student's t-test, and one-way analysis of variance with Tukey's multiple comparisons post-hoc test. $P < 0.05$ was considered to indicate a statistically significant difference.

Results

KRT19 expression is increased in thyroid cancer tissues and is associated with more aggressive clinical characteristics. The TCGA thyroid cancer dataset was downloaded and used for the purposes of this study. As demonstrated in Fig. 1A, the expression profile of genes in the thyroid cancer dataset are presented as a volcano plot (cancer vs. normal), and KRT19 was observed

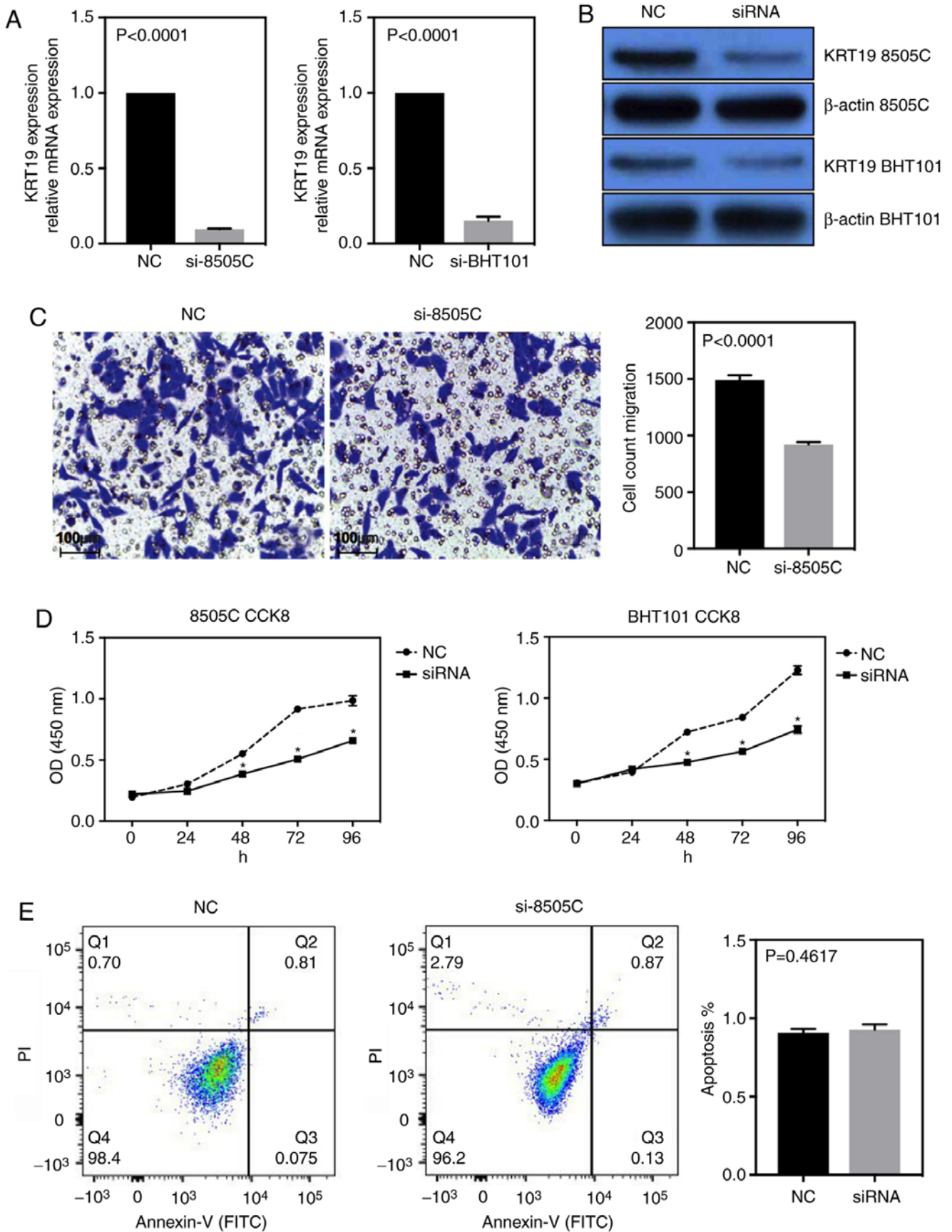


Figure 2. Knockdown of KRT19 expression by RNA interference. The efficiency of siRNA-mediated knockdown was measured by (A) reverse transcription-quantitative PCR and (B) western blot analysis in 8505C and BHT101 cell lines. The mRNA and protein expression levels confirmed the successful knockdown of KRT19 in both cell lines. (C) Thyroid cancer cell migration ability was reduced by KRT19-knockdown. (D) The proliferation of si-KRT19 cells was significantly lower than the control group in both cell lines from 48 h onwards ($P < 0.05$). (E) The apoptotic rate of 8505C cells was measured by flow cytometry, and no significant difference was observed between the si-KRT19 and control groups. KRT19, keratin 19; siRNA, small interfering RNA; FITC, fluorescein isothiocyanate; PI, propidium iodide; OD, optical density.

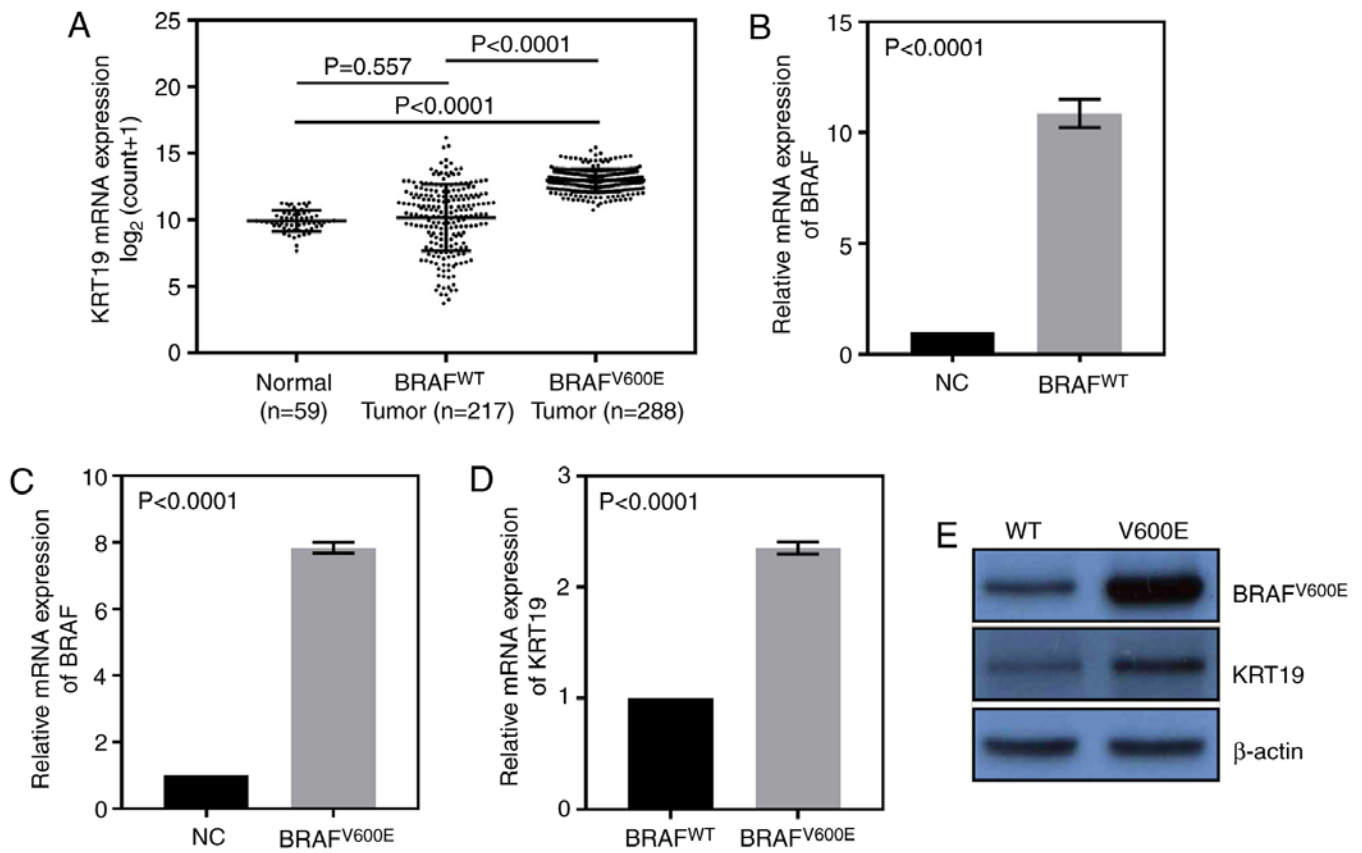


Figure 3. The TCGA_THCA dataset was used for the following analysis. (A) Compared with the BRAF wild type group, the expression of KRT19 was increased in BRAF^{V600E} group, however, not in BRAF wild type group. The (B) wild type BRAF or (C) V600E mutated BRAF overexpression plasmids were transfected into 8505C cells, and may be overexpressed significantly compared with their empty vectors, BRAF^{WT}/BRAF^{V600E}. (D) mRNA and (E) protein expression levels of the BRAF^{V600E} mutation group exhibited higher expression levels of KRT19 in 8505C cells when compared with BRAF wild type group. BRAF, B-Raf Proto-Oncogene, Serine/Threonine Kinase; TCGA, The Cancer Genome Atlas Network; THCA, thyroid cancer; KRT19, keratin 19; WT, wild type.

to be at an upregulated position. As demonstrated in Fig. 1B, KRT19 expression was significantly higher in tumor samples when compared with adjacent normal samples ($P < 0.001$). In addition, KRT19 expression was associated with lymph node metastasis and significantly higher expression levels were observed in the lymph node positive group ($P < 0.001$; Fig. 1C). When patients were categorized by pathological subtype, the follicular subtype (best prognosis) group exhibited the lowest KRT19 expression levels, while the tall cell subtype (worst prognosis) group exhibited the highest KRT19 expression levels (follicular subtype vs. classical subtype, $P < 0.0001$; follicular subtype vs. tall cell subtype, $P < 0.0001$; and classical subtype vs. tall cell subtype, $P = 0.0013$; Fig. 1D). Patients in the TNM stage III-IV group exhibited significantly higher KRT19 expression levels when compared with those in the TNM stage I-II group ($P < 0.001$; Fig. 1F). Similar results were observed for tumor stage analysis ($P < 0.001$; Fig. 1E; Table II).

KRT19-knockdown inhibits thyroid cancer cell proliferation and migration, however, not apoptosis in vitro. To investigate the role of KRT19 in thyroid cancer cell lines the siRNA knockdown system was used. Using two different thyroid cancer cell lines, 8505C and BHT101, the efficiency of siRNA-knockdown was measured by RT-qPCR and western blot analyses (Fig. 2A and B). Using Transwell assays, the migration ability of 8505C cells was also measured. As

demonstrated in Fig. 2C, the migration ability of 8505C cells was significantly reduced following knockdown of KRT19 ($P < 0.001$). The proliferation of thyroid cancer cell lines was then analyzed using a CCK8 assay and fluorescence-activated cell sorting (FACS) in both cell lines. As presented in Fig. 2D, the negative control (NC) groups demonstrated higher cell counts, and the results of FACS analysis indicated no significant alterations in the apoptosis rate between the NC and the si-KRT19 group (Fig. 2E). These results suggest that knockdown of KRT19 decreased the proliferation ability of thyroid cancer cells.

Increased KRT19 expression may be induced by the BRAF^{V600E} mutation. In the TCGA thyroid cancer dataset, it was observed that compared with normal group, the expression of KRT19 was higher only in the BRAF^{V600E} group, however, not the WT group (Fig. 3A). Therefore, BRAF^{V600E} and BRAF^{WT} sequences were then overexpressed in 8505C cells. qRT-PCR results indicated these plasmids could significantly upregulate the expression of BRAF^{WT} or BRAF^{V600E} (Fig. 3B and C). As demonstrated in Fig. 3D and E, the mutation group exhibited higher expression levels of KRT19 when compared with WT group. The results demonstrated that high expression levels of KRT19 were only observed in patients harboring the BRAF^{V600E} mutation, which suggests that BRAF^{V600E} may induce KRT19 expression.

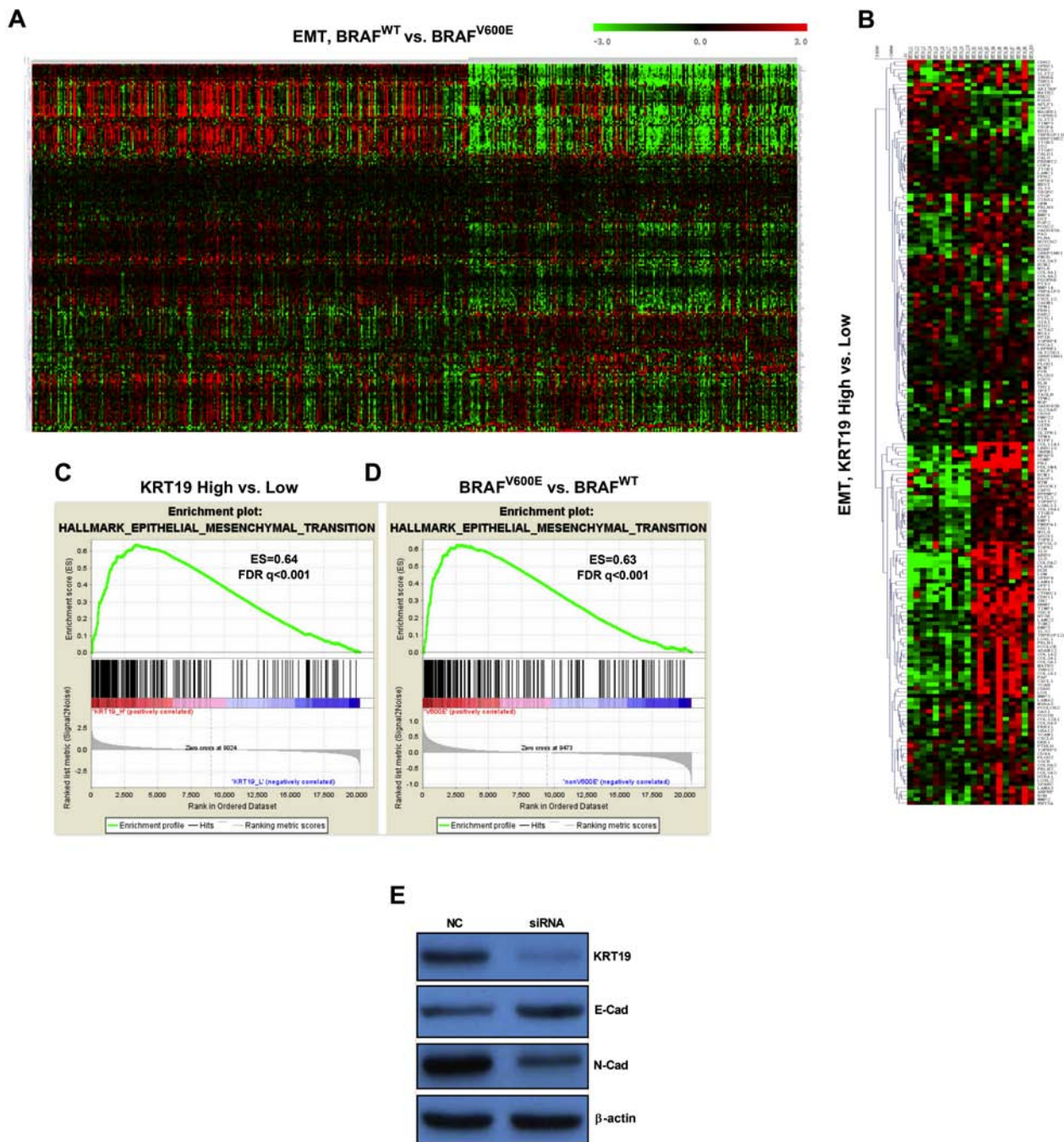


Figure 4. The TCGA_THCA dataset was used for the following analysis. (A and D) Heatmap and GSEA analysis in EMT and BRAF^{V600E} tumor vs. wild type BRAF tumor samples from the TCGA_THCA dataset. (B and C) Heatmap of EMT genes in the top 10 samples exhibiting high KRT19 expression vs. 10 samples with the lowest KRT19 expression from the TCGA dataset. (E) Western blot analysis of EMT markers in the 8505C cell line transfected with controls or si-KRT19. Knockdown of KRT19 was associated with increased E-cadherin and reduced N-cadherin levels when compared with the control group. BRAF, B-Raf Proto-Oncogene, Serine/Threonine Kinase; TCGA, The Cancer Genome Atlas Network; THCA, thyroid cancer; GSEA, Gene Set Enrichment Analysis; EMT, epithelial-mesenchymal-transition; KRT19, keratin-19; siRNA, small interfering RNA; FDR, false discovery rate; ES, enrichment score.

KRT19 exerts its oncogenic activity via EMT. To further investigate the role of KRT19 and the BRAF^{V600E} mutation in thyroid cancer, GSEA was used. Patients from the TCGA thyroid cancer dataset were grouped according to BRAF mutation status (BRAF^{V600E} and WT BRAF groups), and the expression profiles for each group were submitted for GSEA analysis. The results indicated that the BRAF mutation status was significantly associated with EMT (Fig. 4A and D). As

demonstrated in Fig. 4B and C, GSEA was used to analyze the gene expression profiles of the top 10 tumor samples exhibiting the highest levels of KRT19 expression and the top 10 tumor samples exhibiting the lowest expression of KRT19, which revealed EMT. These results suggest that KRT19 may influence EMT. Therefore, the expression of EMT markers was analyzed in 8505C cells, and the results demonstrated that the level of E-cadherin was significantly higher in cells transfected

with si-KRT19, whereas N-cadherin expression levels were significantly lower when compared with the controls.

Discussion

KRT19 is a member of the keratin family of IF proteins, which can be further subdivided into CKs and hair keratins (17). KRT19, as a type I CK, has been reported to be abundantly expressed in epithelial tumor cells and serves as a marker for metastatic tumors (18-20). A previous study suggested that KRT19 expression may be activated by certain signaling pathways. For example, Ju *et al* (10) reported that the erb-b2 receptor tyrosine kinase-2 (ERBB2/HER2)-downstream MEK/ERK signaling pathway stimulated KRT19 expression, and membrane-localized KRT19 can bind to and stabilize HER2 by inhibiting its ubiquitination. In thyroid cancer, increased KRT19 expression was observed in papillary carcinoma when compared with follicular adenoma (21). However, the role of KRT19 in thyroid cancer is currently unclear, so in order to clarify the phenotype of KRT19 in thyroid cancer cell lines and examine its downstream mechanism the present study designed and performed the aforementioned experiments.

The current study presents evidence to suggest that KRT19 expression is elevated in thyroid cancer, which is associated with lymph node metastasis, increased tumor size and advanced TNM stage. Using CCK8 assays and apoptosis analysis, KRT19 knockdown was demonstrated to reduce the proliferation of thyroid cancer cells; however, this was not via the induction of apoptosis. In agreement with the observation that KRT19 was associated with lymph node metastasis, the results of the Transwell assay indicated that KRT19-knockdown decreased the migration of thyroid cancer cells.

BRAF^{V600E} is the most frequently mutated gene in thyroid cancer and, according to the cBioPortal, this mutation is present in ~60% of all cases (22). Therefore, the association between BRAF^{V600E} and KRT19 expression was investigated in the current study. Notably, the expression of KRT19 was observed to be significantly higher in BRAF^{V600E} tumors compared with WT tumors. By transfecting thyroid tumor cells with a plasmid containing BRAF^{V600E}, this mutation was observed to induce the expression of KRT19. Therefore, to the best of our knowledge, this is the first study to report that increased KRT19 expression could be caused by BRAF^{V600E} mutations. Consistent with this hypothesis, GSEA analysis of BRAF^{V600E} vs. WT BRAF thyroid cancer samples indicated EMT. In addition, KRT19 expression was associated with lymph node metastasis in thyroid cancer patients, and GSEA analysis yielded similar results. KRT19 is also known to be involved in EMT (8). Therefore, the level of specific EMT makers were measured in thyroid cancer cell lines in the present study. E-cadherin levels were increased while N-cadherin levels were decreased in thyroid cancer cells transfected with si-KRT19, which indicated that knockdown of KRT19 may influence EMT.

In conclusion, the results of the current study suggest that BRAF^{V600E} mutations may increase the expression of KRT19 in thyroid cancer, which may subsequently lead to lymph node metastasis via induction of EMT.

Acknowledgements

Not applicable.

Funding

The present study was funded by the Health and Family Planning Commission of Shanxi Province (grant no. 2017070).

Availability of data and materials

All data generated or analyzed during the present study are included in this published article.

Authors' contributions

XW and HZ designed the study. XW, CP, TG and XX performed the experiments. YQ and JJ performed the statistical analysis and XW and YQ wrote the manuscript. All authors have read and approved the final manuscript.

Ethics approval and consent to participate

Not applicable.

Patient consent for publication

Not applicable.

Competing interests

The authors declare that they have no competing interests.

References

1. Smith-Bindman R, Lebda P, Feldstein VA, Sellami D, Goldstein RB, Brasic N, Jin C and Kornak J: Risk of thyroid cancer based on thyroid ultrasound imaging characteristics: Results of a population-based study. *JAMA Intern Med* 173: 1788-1796, 2013.
2. Cabanillas ME, McFadden DG and Durante C: Thyroid cancer. *Lancet* 388: 2783-2795, 2016.
3. Pellegriti G, Frasca F, Regalbuto C, Squatrito S and Vigneri R: Worldwide increasing incidence of thyroid cancer: Update on epidemiology and risk factors. *J Cancer Epidemiol* 2013: 965212, 2013.
4. Randle RW, Bushman NM, Orne J, Balentine CJ, Wendt E, Saucke M, Pitt SC, Macdonald CL, Connor NP and Sippel RS: Papillary thyroid cancer: The good and bad of the 'good cancer'. *Thyroid* 27: 902-907, 2017.
5. Karantza V: Keratins in health and cancer: More than mere epithelial cell markers. *Oncogene* 30: 127-138, 2011.
6. Paiva F, Duarte-Pereira S, Costa VL, Ramalho-Carvalho J, Patrício P, Ribeiro FR, Lobo F, Oliveira J, Jerónimo C and Henrique R: Functional and epigenetic characterization of the KRT19 gene in renal cell neoplasms. *DNA Cell Biol* 30: 85-90, 2011.
7. Cen D, Chen J, Li Z, Zhao J and Cai X: Prognostic significance of cytokeratin 19 expression in pancreatic neuroendocrine tumor: A meta-analysis. *PLoS One* 12: e0187588, 2017.
8. Takano M, Shimada K, Fujii T, Morita K, Takeda M, Nakajima Y, Nonomura A, Konishi N and Obayashi C: Keratin 19 as a key molecule in progression of human hepatocellular carcinomas through invasion and angiogenesis. *BMC Cancer* 16: 903, 2016.
9. Masai K, Nakagawa K, Yoshida A, Sakurai H, Watanabe S, Asamura H and Tsuta K: Cytokeratin 19 expression in primary thoracic tumors and lymph node metastases. *Lung Cancer* 86: 318-323, 2014.
10. Ju JH, Oh S, Lee KM, Yang W, Nam KS, Moon HG, Noh DY, Kim CG, Park G, Park JB, *et al*: Cytokeratin19 induced by HER2/ERK binds and stabilizes HER2 on cell membranes. *Cell Death Differ* 22: 665-676, 2015.
11. Edge SB and Compton CC: The American Joint Committee on Cancer: the 7th edition of the AJCC cancer staging manual and the future of TNM. *Ann Surg Oncol* 17: 1471-1474, 2010.

12. Li B and Dewey CN: RSEM: Accurate transcript quantification from RNA-Seq data with or without a reference genome. *BMC Bioinformatics* 12: 323, 2011.
13. Subramanian A, Tamayo P, Mootha VK, Mukherjee S, Ebert BL, Gillette MA, Paulovich A, Pomeroy SL, Golub TR, Lander ES and Mesirov JP: Gene set enrichment analysis: A knowledge-based approach for interpreting genome-wide expression profiles. *Proc Natl Acad Sci USA* 102: 15545-15550, 2005.
14. Mootha VK, Lindgren CM, Eriksson KF, Subramanian A, Sihag S, Lehar J, Puigserver P, Carlsson E, Ridderstråle M, Laurila E, *et al*: PGC-1alpha-responsive genes involved in oxidative phosphorylation are coordinately downregulated in human diabetes. *Nat Genet* 34: 267-273, 2003.
15. Ohtsuka T, Sakaguchi M, Yamamoto H, Tomida S, Takata K, Shien K, Hashida S, Miyata-Takata T, Watanabe M, Suzawa K, *et al*: Interaction of cytokeratin 19 head domain and HER2 in the cytoplasm leads to activation of HER2-Erk pathway. *Sci Rep* 6: 39557, 2016.
16. Livak KJ and Schmittgen TD: Analysis of relative gene expression data using real-time quantitative PCR and the 2(-Delta Delta C(T)) method. *Methods* 25: 402-408, 2001.
17. Saha SK, Choi HY, Kim BW, Dayem AA, Yang GM, Kim KS, Yin YF and Cho SG: KRT19 directly interacts with β -catenin/RAC1 complex to regulate NUMB-dependent NOTCH signaling pathway and breast cancer properties. *Oncogene* 36: 332-349, 2017.
18. Stathopoulos EN, Sanidas E, Kafousi M, Mavroudis D, Askoxylakis J, Bozionelou V, Perraki M, Tsiftsis D and Georgoulas V: Detection of CK-19 mRNA-positive cells in the peripheral blood of breast cancer patients with histologically and immunohistochemically negative axillary lymph nodes. *Ann Oncol* 16: 240-246, 2005.
19. Yang XR, Xu Y, Shi GM, Fan J, Zhou J, Ji Y, Sun HC, Qiu SJ, Yu B, Gao Q, *et al*: Cytokeratin 10 and cytokeratin 19: Predictive markers for poor prognosis in hepatocellular carcinoma patients after curative resection. *Clin Cancer Res* 14: 3850-3859, 2008.
20. Chen TF, Jiang GL, Fu XL, Wang LJ, Qian H, Wu KL and Zhao S: CK19 mRNA expression measured by reverse-transcription polymerase chain reaction (RT-PCR) in the peripheral blood of patients with non-small cell lung cancer treated by chemo-radiation: An independent prognostic factor. *Lung Cancer* 56: 105-114, 2007.
21. Arcolia V, Journe F, Renaud F, Leteurtre E, Gabius HJ, Rimmelink M and Saussez S: Combination of galectin-3, CK19 and HBME-1 immunostaining improves the diagnosis of thyroid cancer. *Oncol Lett* 14: 4183-4189, 2017.
22. Cerami E, Gao J, Dogrusoz U, Gross BE, Sumer SO, Aksoy BA, Jacobsen A, Byrne CJ, Heuer ML, Larsson E *et al*: The cBio cancer genomics portal: An open platform for exploring multi-dimensional cancer genomics data. *Cancer Discov* 2: 401-404, 2012.



This work is licensed under a Creative Commons Attribution-NonCommercial-NoDerivatives 4.0 International (CC BY-NC-ND 4.0) License.